Automated diagnosis of COVID-19 pneumonia from X-ray and CT images

Farima Fatahi Bayat, Runchu Ma, Sara Shoouri, Jiahong Xu

{farimaf, runma, sshoouri, jiahongx}@umich.edu

Abstract

As COVID-19 spreads around the world, increasing demand for COVID-19 testing burdens health care workers. Researchers started to utilize machine learning techniques to identify COVID-19 cases using CT scans or X-rays to help this situation. Deep classification models, such as convolutional neural networks (CNNs), require large-scale datasets to be trained in order to achieve a reasonably accurate model. Since the number of X-ray samples related to COVID-19 is limited, in this study, reliable pre-trained deep learning algorithms will be applied to achieve an automatic diagnosis of COVID-19 pneumonia from digital chest X-ray images (this method has been called Transfer learning). We have also investigated the current dataset issues such as biases and other existing factors to ensure the model will work properly.

Index Terms: COVID-19 pneumonia, convolutional neural networks, Transfer Learning, Chest X-ray image

1. Introduction

As WHO declares COVID-19 as a global pandemic, it affects many people's daily lives. As of Mar. 30 th, there has been 127,349,248 confirmed cases and 2,787,593 death globally reported by WHO [3]. With the growing number of cases, there are increasing demands for fast and accurate detections of COVID-19. A standard testing method is called reverse transcription-polymerase chain reaction (RT-PCR). However, the test alone takes a long time to produce a result [27]. Although this type of testing provides higher accuracy, it is uncomfortable for the patient and dangerous for the operator due to aerosol emission during the procedure [31].

Therefore, automatic detection using chest X-rays can be a crucial tool in the emergency setting. It allows a first rough evaluation, which can be obtained when the patients are lying on a bed connecting to portable devices and needs a limited exposure for the operator.

Given these imaging techniques, machine learning methods can automate the detection process and support human decisions. As the machine learning-based approaches become popular in medical image classification problems, one naturally thinks that this method can be used to identify COVID-19 cases.

We propose a method for screening COVID-19 from patients' chest medical images using machine learning in this work. For this goal, we present a classification model that gets the X-ray image and Computer Tomography (CT) scan of a patient's chest as input and predicts the presence of the COVID-19 case or non-COVID-19 case.

In this work, there are a few challenges that we want to investigate:

- **Transfer Learning:** As [31] stated, although Transfer learning can be effective for COVID-19 detection, we need to make sure that the pre-trained models do not have biases in their models and they do not design for a particular task. This step is crucial to make sure that the feature extractor works well on the chest X-ray images.
- **Size of dataset:** The size of the dataset is relatively small, and it can cause an over-fitting phenomenon. We have considered data augmentation to prevent this issue.
- **Biases in the dataset:** Due to the public dataset's limited availability, the chest X-ray images do not contain various ages and genders. Moreover, the contrasts and the lighting are not distributed equally on the different classes, and some of the pictures have textual labeling. We have applied pre-processing algorithms mentioned in section 2.2 to correct the biases for later issues.

2. Proposed Method

In this section, we are going to describe the proposed deep learning approach. The overall pipeline for the proposed method has been shown in Fig. 1. It mainly consists of data collection, image pre-processing, and classification model obtained with Transfer learning, which are described in detail in sections 2.1, 2.2, and 2.3, respectively.

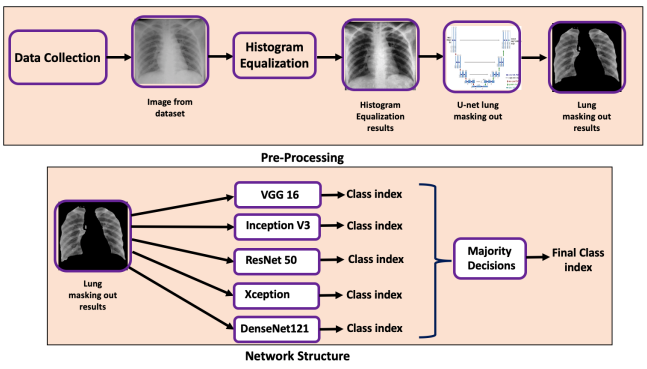

Figure 1: *Overall Pipeline of the proposed method.*

2.1. Data Collection

This section describes five datasets that have been investigated to be considered in this work. In what follows, we list out each dataset's properties and determine the selected dataset for our work.

2.1.1. COVID-CT dataset

For this dataset, [32], CT images of patients with COVID-19 were collected from scientific preprints, posted from January 19th to March 25th. Some of the images were then denoted by hospital radiologists. A total of 349 CT images from 216 covid patients exist in this dataset.

For non-covid instances, the collectors used four other datasets (LUNA, MedPix PMC, Radiopaedia). This collection is composed of 463 non-covid images from 55 patients. However, these images represent both healthy patients and patients with other pulmonary diseases such as lung cancer.

2.1.2. SARS-CoV-2 CT-scan dataset

This dataset [29] was collected from hospitals of Sao Paulo, Brazil. It consists of 2482 CT scans from 120 patients in total. There are 1252 CT images from 60 patients infected with SARS-CoV-2 and 1230 CT scan images from 60 non-infected patients, possibly with other pulmonary diseases (such as lung cancer).

2.1.3. COVID-19 Image Data Collection

This dataset [12] is the first public COVID-19 chest X-ray image data collection that has been assembled using databases on websites such as Radiopaedia.org [5], the Italian Society of Medical and Interventional Radiology [29], and the Hannover Medical School [16]. It is collected either manually or using scrapers. The dataset consists of 679 frontal chest X-ray images from 412 patients in total. There are 468 COVID-19 instances and 211 non-covid instances. Analogous to previous datasets, the non-covid images present other pulmonary diseases categorized into viral, bacterial, fungal, lipoid, aspiration, and unknown.

2.1.4. COVID-CT-MD dataset

This dataset [7] is collected in Babak Imaging Center, Tehran, Iran. It contains volumetric chest CT scans of 171 patients who test positive for COVID-19 infection from February 2020 to April 2020. It also consists of images from 60 patients with Community Acquired Pneumonia (CAP) and 76 healthy people. Each patient has several CT-scan slices in DICOM format. We did not consider this dataset because each patients' CT-scan set contains selected parts of images, and sometimes the whole set of CT-scan images was not available.

2.1.5. COVID-19 Radiography dataset

This dataset [11, 25], is the winner of the COVID-19 dataset Award, which is awarded by the Kaggle community. The chest X-ray images of this dataset are collected from four major data sources: Italian Society of Medical and Interventional Radiology (SIRM) COVID-19 database [6], Novel Corona Virus 2019 dataset [2], COVID-19 positive chest x-ray images from different articles ([30] and [5]), and COVID-19 Chest imaging at thread reader [4].

The dataset has a total number of 3616 COVID-19 positive CXR images. There are 10,192 Normal, 6012 Lung Opacity (Non-COVID lung infection), and 1345 Viral Pneumonia images.

After investigating the pros and cons of the datasets mentioned above, we selected the COVID-19 Radiography dataset as it has plenty of high-quality CXR instances for both covid and normal (healthy) cases. We apply different pre-processing methods to all COVID instances of this dataset and 3616 normal instances to generate a balanced dataset for the rest of this work.

2.2. Pre-processing

As we have already stated, image pre-processing can be considered as an essential step to ensure that the classification model will discriminate different classes without considering biases in the dataset. Image pre-processing contains two main subsections: histogram equalization and Lung segmentation, which are investigated in detail in the following subsections.

2.2.1. ***Histogram equalization:***

The purpose of the Histogram equalization is to remove the biases exciting in the dataset. The contrast for X-ray and CT-scan images depends on various reasons, mainly depending on subject contrast or other factors [31]. For instance, in the chosen dataset, "COVID" X-ray images have lower contrast levels than the "Normal" X-ray images. This phenomenon can lead to generate biases on the Neural Network models and make the Neural Network learn the existing bias as one of the distinguishing factors for classifying the dataset.

We have applied Histogram equalization to all images to guarantee a uniform dynamic image in order to deal with this issue. We have used "Contrast Limited Adaptive Histogram Equalization—CLAHE" [34]. CLAHE method creates non-overlapping sub-images and blocks for a given image, applies Histogram equalization to each block, and finally clips the contrast amplification to a specific value. The clipping of contrast amplification improves the noise reduction on images. There are two hyper-parameters for CLAHE algorithm, which are **tile size** and **clip limit**. Tile size is the neighborhood region's size, and clip limit is the value at which the histogram is clipped. The results for Histogram equalization are shown in 4.1.

2.2.2. ***Lung segmentation:***

The lung segmentation for X-ray images can reduce the bias sources such as the texts available on the images or the medical devices attached to the sick patients [31]. We have developed a U-net structure for masking out the lung segments [19].

• **U-net architecture:**

U-net is a convolutional neural network developed

for biomedical image segmentation, which is fast and relies on a small annotated training dataset [26]. It is widely used in the area of semantic segmentation of cell microscopy images [26], CT-scans [8] and X-ray images [31]. Some other neural networks are proposed [21, 33] based on the U-net.

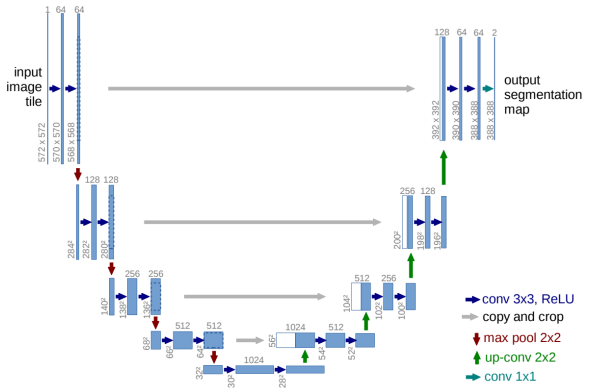

Figure 2: *U-net architecture [26]*

The structure of the U-net is shown in Fig. 2. The input of the U-net is a raw image, and the output is a segmentation mask. It consists of two parts: a contracting path (left side) and an expensive path (right side). The contracting path extracts features from the input images as a standard convolutional neural network. The expansive path halves the feature channels, unsamples the feature maps, and concatenates the high-resolution features from the contracting path with the feature maps. The concatenation mitigates the loss of border information due to the down-convolution operation in the contracting path. The output of U-net consists of two channels: background and foreground class.

• **Training process of U-net and masking out the lungs:**

We have used two datasets, which are publicly available datasets from Montgomery County, Maryland, and Shenzhen Hospital in China [1]. Segmented lung masks are manually labeled for both of these datasets, and this is why we use different training datasets than our chosen data mentioned in section 2.1 for this part. The overall amount of images is 800, and the whole dataset is randomly divided into train dataset (which is 0.8 of total), validation dataset (which is 0.1 of train dataset), and test dataset. We have applied padding, cropping, and resizing to $512 * 512$ to all of the dataset images. We have also combined the left and right lung masks for the images. Fig .3 shows one of the dataset's images with the manually labeled lung segmentation after combing the left and right masks.

As we have stated, the U-net structure has an encoder and a decoder path. The expansive path that performs the Upsampling of the feature map is combined with high-resolution features from the contracting path to generate the precise lung masks, and this is why we choose the U-net model as our "lung segmentation" model.

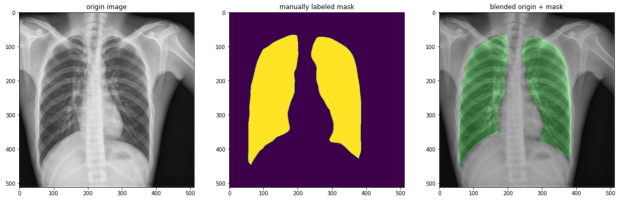

Figure 3: *Left image: Original Image. Middle image: Manually labeled mask. Right image: Combination of mask and original image.*

Every image consists of pixels, and we consider the lung mask segmentation as a binary classification for each pixel. As a result, we have applied the Softmax function to each pixel and computed the negative log-likelihood loss between the output of Softmax and the labeled mask as the U-net's loss function.

2.3. Network Architecture

To solve this problem, we use a popular strategy that is called "transfer learning." Transfer learning is a strategy in which a model trained on a tremendous amount of data is used as a pre-trained model for a different task. We select few last layers of a pre-trained model and fine-tune these layers' parameters using our dataset. The rest of the pre-trained model layers remain frozen, and their weights will be used.

Our plan is to use the five popular network models, which are InceptionV3, VGG16, DenseNet121, Xception, and ResNet50 for image classification. The final output is then the combination of the predicted values of these five networks using "majority voting" [23]. We use this approach to mitigate the individual models' error to predict the valid class label.

2.3.1. Dataset

We first split the pre-processed dataset into three categories: train set, valuation set, and test set. To create these three sets, we first shuffle the COVID and Normal instances. Then, we randomly pick 10% of the data, which is 723 images for the test set. From what remains, we randomly choose 90% of the data (5859 images) for the training set and 10% of the data (650 images) for the validation set. We plan to use K-fold validation to enhance the accuracy.

2.3.2. CNN models

VGG16 [28]: is a convolution neural net (CNN) architecture that was introduced to win ILSVR (Imagenet) competition in 2014. It consists of a stack of convolutional layers (known as feature extractor). Three fully-connected (FC) layers which form the classifier part of the model follow the feature extractor: the first two have 4096 channels each, the third performs 1000-way image classification and contains 1000 channels. The network is

trained on the ImageNet dataset [13]. We replace the last FC layer with a two-channel linear layer such that it classifies the images as either COVID or normal. Then, we freeze the feature extractor's parameters and only update the parameters in the classifier part of the model during training.

ResNet18 [14]: is a residual learning framework that won 1st place on the ILSVRC 2015 classification task. This network has 18 layers. It consists of one convolution and pooling step followed by four layers of similar behavior. Each of the layers follows the same pattern. They perform 3x3 convolution with a fixed feature map dimension (F) [64, 128, 256] respectively, bypassing the input every two convolutions. In the end, one fully connected layer which has 1000 channels is used for 1000-way classification. We use the pre-trained version of this model and do the same process as VGG16 to fine-tune the ResNet18 model. We adapted the smaller version of this residual network (ResNet18) for faster training, but we will use ResNet50 for higher performance in the future.

2.4. Evaluation

As we will evaluate a medical screening system and compare our model to other state-of-the-art methods in the literature, the useful evaluation metrics are Accuracy, Precision, Recall, and F-1 score. However, we stick to the accuracy of the classification models that define the model's ability to classify COVID and Normal cases correctly for this step. We use validation accuracy to tune the CNN models' hyper-parameters, as discussed in Section 4.4.

3. Related Work

During the outbreak of COVID-19, X-ray images and CT scans play essential roles in detecting injected patients. This leads to the research of the detection model for COVID-19 patterns in CT images [22]. Transfer learning is universally implemented in the classification of different kinds of pneumonia-injected patients [27, 22]. The model based on ResNet50 is presented in [15], and the researchers established the model based on EfficientNets in [27].

Moreover, the automatic diagnosis of different kinds of pneumonia based on chest X-ray images has received many interests. Pre-trained and untrained GoogleNet, and AlexNet have been implemented to diagnose tuberculosis from chest radiographs [20]. Also, [10] shows that the ensemble classification method could improve the performance. The new architectures of deep CNNs are proposed to prompt the classification accuracy [24].

However, due to the small datasets for COVID cases and the lack of information about patients' ages and genders, hidden biases are difficult to correct. Diverse light conditions, contrast rates among different X-ray images, and textual annotations could make the training process even harder. Tartaglione [31] provides the idea of histogram equalization and lung segmentation to reduce some of the biases. This method is used in this project because the images of COVID cases tend to be in low contrast and contain some annotations and marks. Different neural network models have been used for lung segmentation [9, 17], including the application of the U-net [31].

4. Experimental results

4.1. Results for Histogram Equalization

We have found that **tile size=4** and **clip limit=4** give us the best performance according to the lung segmentation mentioned in 2.2.2. Fig. 4 shows one of the COVID images before and after applying the Histogram equalization. It can be found out that the contrast on the right image is much higher than the contrast on the left image, and this can help the "Lung segmentation model" to recognize and generate the lung masks much better.

Figure 4: *Left image: Original COVID image. Right image: COVID image after applying the Histogram Equalization with "tile size=4" and "clip limit=4".*

4.2. Results for Lung Segmentation

We have trained the U-net model using the **Adam** optimizer with **learning rate of 0.0005**, **batch size of 4**, and **67 epochs**. We have initialized the weights with the pre-trained Vgg11 model, as it has a similar structure to the U-net. Moreover, this fine-tuning can help the model to converge faster.

For evaluating the model's performance, we have used two various metrics, which are Dice and Jaccard. Both of these metrics almost compute the overlap between ground truth and computed mask.

Dice coefficient can be written as follows [19]:

$$DICE = \frac{|S \bigcap GT|}{|S| + |GT|} = \frac{2 * |TP|}{2 * |TP| + |FN| + |FP|} \quad (1)$$

Where, GT is the ground truth and S is the computed mask. Also, TP, FN, and FP are True positive, False Negative , and False Positive results, respectively.

Moreover, Jaccard index is Intersection Over Union and can be written as follows [18]:

$$J(S, GT) = \frac{|S \bigcap GT|}{|S \bigcup GT|} = \frac{|S \bigcap GT|}{|S| + |GT| - |S \bigcap GT|} \quad (2)$$

A model with a higher DICE coefficient and Jaccard index indicates better performance in masking out the lungs.

Fig. 5, shows the values of loss function for training and validation dataset, and DICE coefficient, Jaccard index for validation dataset. From the figure, we can find out that the DICE coefficient and Jaccard index reach almost close to 1 after few epochs, and the training and validation losses quickly converge.

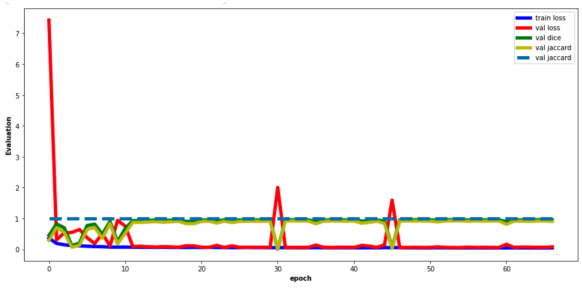

Figure 5: *Evaluation results for lung segmentation* .

Additionally, Fig. 6 shows three different images of the dataset. The "red area", "green area", and "yellow area" are the predicted mask, ground truth mask, and the intersection area, respectively. Also, the DICE coefficient and Jaccard index for each image have been computed and shown.

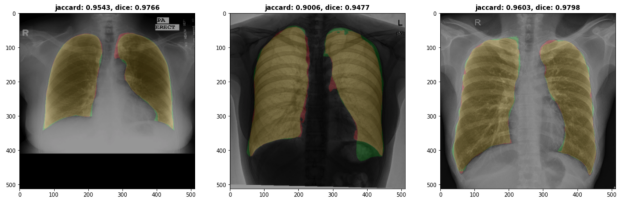

Figure 6: *Obtained results for three different images. Left Image: Jaccard* 0.9543*, DICE* 0.9766*. Middle Image: Jaccard* 0.9006*, DICE* 0.9477*. Right Image: Jaccard* 0.9603*, DICE* 0.9798*.*

4.3. Combining Histogram Equalization and Masking out the lungs:

Given the U-net result with and without Histogram Equalization, we select in between the sets of data to achieve better performance in the classification. Images with histogram equalization often reveal more prominent contrast between the background and lung details. However, these images often display lung fibers more clearly at the expense of revealing the chest bones with equal intensity. Therefore, these images might misdirect the network to learn about chest bone patterns instead of the fibers. On the other hand, images without histogram equalization sometimes do not show the fibers clearly, making the network harder to train. These two types of images are shown in Fig. 7.

To take both methods' advantages, we decide to compare the sets of images with and without histogram equalization and use the one that we think will result in the best

Figure 7: *Left: Image with Histogram Equalization, Right: Image without Histogram Equalization*

performance. This task is done manually to achieve the best result.

4.4. Training CNN models

4.4.1. VGG16

Before the training process, we conducted a sanity check, where we tried to overfit the model to a small set of images. The small training set contains 200 pictures, and the validation set has 50 photos. Fig. 8 shows the accuracy and the loss of each epoch. The leap between the training accuracy and the validation accuracy shows that the model performs as our expectations.

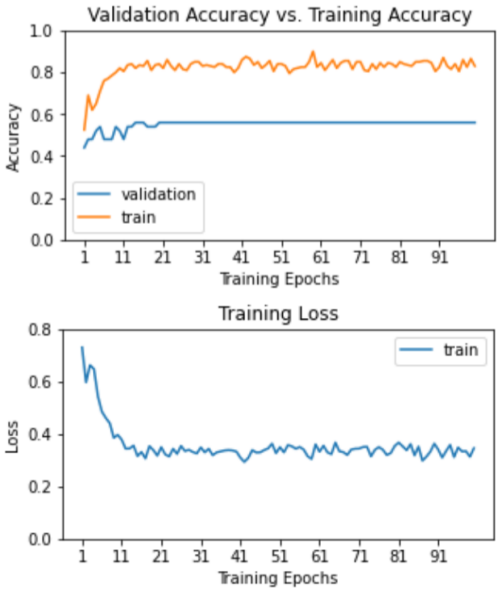

Figure 8: *Overfit of a small dataset: Comparison of validation accuracy and training accuracy (upper); training loss (lower)*

Then, we proceed and feed the whole training dataset to the system and monitor the validation performance for hyper-parameter tuning. The performances of the VGG16 model using different configurations are shown in Table 1. As shown in this table, using the **learning rate of** 0.001 and a **step-size of** 25 for the learning rate scheduler reveals the best performance when training for

75 epochs. The test accuracy using the chosen setting is 85.53%. We use **SGD** (stochastic gradient decent) optimizer and the StepLR learning scheduler [1] from the optim module of torch package. The step size is the period of learning rate decay.

4.4.2. ResNet18

Using a similar method as applied to the VGG16 network, we trained ResNet18 using pre-trained weights. The following results are obtained using ResNet 18. We set the **learning rate at 0.001** and **momentum at 0.9**. We found that the final validation accuracy is 79.38% and the test accuracy is 81.05%. Fig. 9 shows the model's training and validation accuracy curves and training loss graphs. It can be seen, we have faced the over-fitting issue, and this can be solved by applying different data augmentation, K-fold validation, and cleaning the dataset, which will be done in future steps.

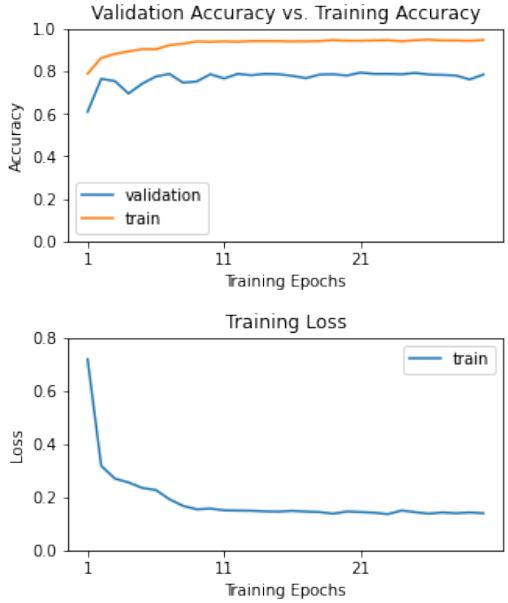

Figure 9: *Training and validation accuracy for ResNet18 (upper); training loss for ResNet18 (lower)*

5. Future milestone

Date	Milestone
4/02	Fine-tuning of the neural network
4/09	Error analysis & dataset clean-up
4/16	Fine-tuning of the neural network
4/23	Testing & evaluation
4/30	Finish the final report

[1] https://pytorch.org/docs/stable/optim.html.

6. Conclusions

In conclusion, we were able to complete all the necessary pre-processing work needed to train the network. Specifically, we accomplished data collection, applying trained U-net to mask out lungs, applying histogram equalization to contrast the lungs' details from the background, and selecting the best resulting images. Moreover, we have done some preliminary training for the classification model.

As we have seen from the previous section, both VGG16 and ResNet have faced the over-fitting issue. We will need to do different hyper-parameters tuning, cleaning the dataset, and K-fold validation to solve this problem.

We will do transfer learning on networks to classify images with COVID-19 and normal labels and classify the test data set in later work. We will evaluate the result from different networks and pick the most reasonable result based on our evaluation criteria. Our goal for the project is to train a network using transfer learning to achieve a high accuracy in classifying CT-images that belongs to COVID-19 patients.

7. Author Contributions

Farima Fatahi Bayat:

Collected Data and came up with a road map for data pre-processing to be followed by other team members; trained different variations of VGG16; wrote the following sections of the report: Data Collection (2.1.), Network Architecture (2.3.1 and 2.3.2), Evaluation (2.4), Training CNN models (VGG16 (4.4.1) second part).

Runchu Ma:

Helping with data collections, Data analysis work for with and without histogram equalization result, training ResNet for classification; wrote the following section of report: introduction, combine histogram equalization and masking out the lung, ResNet18 (4.4.2), and conclusion

Sara Shoouri:

Gathered the dataset and masking labels for the "lung segmentation", wrote the U-net lung masking out script, and trained the model for 67 epochs. Also, wrote the Histogram equalization code and generated the lung masking for images with and without histogram Equalization. Moreover, wrote the following sections: Histogram equalization (2.2.1), Training process of U-net and masking out the lungs (2.2.2), Results for Histogram Equalization (4.1), Results for Lung Segmentation (4.2), Abstract, and Figure 1.

Jiahong Xu:

Tried to apply an open source code of U-net to perform lung segmetion; wrote a daft script for the training process of VGG16; wrote the report of the following parts:

Learning Rate	LR_scheduler step size	validation accuracy(%)
0.002	7	82.3
0.002	25	81.6
0.001	25	**86.63**

Table 1: *VGG16 performance on the pre-processed COVID dataset*

U-net architecture, related work, Training CNN models (VGG16 (4.4.1) first part), and Network structure (2.3).

8. References

[1] Montgomery County and Shenzhen Hospital. http://openi.nlm.nih.gov/imgs/collections/ChinaSet_AllFiles.zip.

[2] Novel Corona Virus 2019 dataset. https://github.com/ieee8023/covid-chestxray-dataset. [Online].

[3] WHO. https://covid19.who.int/.

[4] C. imaging. https://threadreaderapp.com/thread/1243928581983670272.html, 2020.

[5] Radiopedia. https://radiopaedia.org/, 2020. [Online].

[6] SIRM database. https://sirm.org/category/senza-categoria/covid-19/, 2020. [Online].

[7] P. Afshar, S. Heidarian, N. Enshaei, F. Naderkhani, M. J. Rafiee, A. Oikonomou, F. B. Fard, K. Samimi, K. N. Plataniotis, and A. Mohammadi. Covid-ct-md: Covid-19 computed tomography (ct) scan dataset applicable in machine learning and deep learning, 2020.

[8] B. Ait Skourt, A. El Hassani, and A. Majda. Lung ct image segmentation using deep neural networks. *Procedia Computer Science*, 127:109–113, 2018.

[9] S. Candemir, S. Jaeger, K. Palaniappan, J. P. Musco, R. K. Singh, Z. Xue, A. Karargyris, S. Antani, G. Thoma, and C. J. McDonald. Lung segmentation in chest radiographs using anatomical atlases with nonrigid registration. *IEEE transactions on medical imaging*, 33(2):577—590, February 2014.

[10] V. Chouhan, S. K. Singh, A. Khamparia, D. Gupta, P. Tiwari, C. Moreira, R. Damaševičius, and V. H. C. de Albuquerque. A novel transfer learning based approach for pneumonia detection in chest x-ray images. *Applied Sciences*, 10(2), 2020.

[11] M. E. H. Chowdhury, T. Rahman, A. Khandakar, R. Mazhar, M. A. Kadir, Z. B. Mahbub, K. R. Islam, M. S. Khan, A. Iqbal, N. A. Emadi, M. B. I. Reaz, and M. T. Islam. Can ai help in screening viral and covid-19 pneumonia? *IEEE Access*, 8:132665–132676, 2020.

[12] J. P. Cohen, P. Morrison, L. Dao, K. Roth, T. Q. Duong, and M. Ghassemi. Covid-19 image data collection: Prospective predictions are the future. *arXiv 2006.11988*, 2020.

[13] J. Deng, W. Dong, R. Socher, L.-J. Li, K. Li, and L. Fei-Fei. Imagenet: A large-scale hierarchical image database. In *2009 IEEE conference on computer vision and pattern recognition*, pages 248–255. Ieee, 2009.

[14] K. He, X. Zhang, S. Ren, and J. Sun. Deep residual learning for image recognition, 2015.

[15] X. He, X. Yang, S. Zhang, J. Zhao, Y. Zhang, E. Xing, and P. Xie. Sample-efficient deep learning for covid-19 diagnosis based on ct scans. *medRxiv*, 2020.

[16] H. L. Hinrich Winther and B. Meyer. Covid-19 image repository, 2020.

[17] S. Hu, E. A. Hoffman, and J. M. Reinhardt. Automatic lung segmentation for accurate quantitation of volumetric x-ray ct images. *IEEE Transactions on Medical Imaging*, 20(6):490–498, 2001.

[18] V. Iglovikov and A. Shvets. Ternausnet: U-net with vgg11 encoder pre-trained on imagenet for image segmentation. *arXiv preprint arXiv:1801.05746*, 2018.

[19] J. Islam and Y. Zhang. Towards robust lung segmentation in chest radiographs with deep learning. *arXiv preprint arXiv:1811.12638*, 2018.

[20] P. Lakhani and B. Sundaram. Deep learning at chest radiography: Automated classification of pulmonary tuberculosis by using convolutional neural networks. *Radiology*, 284(2):574–582, 2017.

[21] X. Li, H. Chen, X. Qi, Q. Dou, C.-W. Fu, and P. A. Heng. H-denseunet: Hybrid densely connected unet for liver and tumor segmentation from ct volumes, 2018.

[22] H. S. Maghdid, A. T. Asaad, K. Z. Ghafoor, A. S. Sadiq, and M. K. Khan. Diagnosing covid-19 pneumonia from x-ray and ct images using deep learning and transfer learning algorithms, 2020.

[23] A. K. Mishra, S. K. Das, P. Roy, and S. Bandyopadhyay. Identifying covid19 from chest ct images: a deep convolutional neural networks based approach. *Journal of Healthcare Engineering*, 2020, 2020.

[24] U. J. M. D.-U. J. Okeke Stephen, Mangal Sain. An efficient deep learning approach to pneumonia classification in healthcare. *Journal of Healthcare Engineering*, 2019, 2019.

[25] T. Rahman, A. Khandakar, Y. Qiblawey, A. Tahir, S. Kiranyaz, S. B. Abul Kashem, M. T. Islam, S. Al Maadeed, S. M. Zughaier, M. S. Khan, and M. E. Chowdhury. Exploring the effect of image enhancement techniques on covid-19 detection using chest x-rays images. *Computers in Biology and Medicine*, page 104319, 2021.

[26] O. Ronneberger, P. Fischer, and T. Brox. U-net: Convolutional networks for biomedical image segmentation. *CoRR*, abs/1505.04597, 2015.

[27] P. Silva, E. Luz, G. Silva, G. Moreira, R. Silva, D. Lucio, and D. Menotti. Covid-19 detection in ct images with deep learning: A voting-based scheme and cross-datasets analysis. *Informatics in Medicine Unlocked*, 20:100427, 2020.

[28] K. Simonyan and A. Zisserman. Very deep convolutional networks for large-scale image recognition, 2015.

[29] E. Soares, P. Angelov, S. Biaso, M. H. Froes, and D. K. Abe. Sars-cov-2 ct-scan dataset: A large dataset of real patients ct scans for sars-cov-2 identification. *medRxiv*, 2020.

[30] R. M. M. Z. B. M. K. R. I. M. S. K. A. I. N. A.-E. T. R. Muhammad E. H. Chowdhury, A. Khandakar and M. B. I. Reaz. Covid-19 chest x-ray database, 2020. [Online].

[31] E. Tartaglione, C. A. Barbano, C. Berzovini, M. Calandri, and M. Grangetto. Unveiling covid-19 from chest x-ray with deep learning: a hurdles race with small data. *International Journal of Environmental Research and Public Health*, 17(18):6933, 2020.

[32] X. Yang, X. He, J. Zhao, Y. Zhang, S. Zhang, and P. Xie. Covid-ct-dataset: A ct scan dataset about covid-19, 2020.

[33] Z. Zeng, W. Xie, Y. Zhang, and Y. Lu. Ric-unet: An improved neural network based on unet for nuclei segmentation in histology images. *IEEE Access*, 7:21420–21428, 2019.

[34] J. B. Zimmerman, S. M. Pizer, E. V. Staab, J. R. Perry, W. McCartney, and B. C. Brenton. An evaluation of the effectiveness of adaptive histogram equalization for contrast enhancement. *IEEE Transactions on Medical Imaging*, 7(4):304–312, 1988.